Lehigh University
Lehigh Preserve

Fritz Laboratory Reports

Civil and Environmental Engineering

1981

Comparison of measured and theoretical forces in lateral bracing members, July 1981

Dennis R. Mertz

J. Hartley Daniels

Lehigh University

High Cycle Fatigue of Welded Bridge Details

COMPARISON OF MEASURED AND THEORETICAL FORCES IN LATERAL BRACING MEMBERS

by

Dennis R. Mertz
J. Hartley Daniels

Fritz Engineering Laboratory

Report No. 386-6 (81)

Technical Report Documentation Page

1. Report No.	2. Government Accession No.	3. Recipient's Catalog No.
4. Title and Subtitle Comparison of Measured and Theoretical Forces in Lateral Bracing Members		5. Report Date July 1981
		6. Performing Organization Code
7. Author(s) Dennis R. Mertz and J. Hartley Daniels		8. Performing Organization Report No. Fritz Lab No. 386-6(81)
9. Performing Organization Name and Address Fritz Engineering Laboratory #13 Lehigh University Bethlehem, Pennsylvania 18015		10. Work Unit No. (TRAIS)
		11. Contract or Grant No. 72-3 (FCP No. 45F2212)
12. Sponsoring Agency Name and Address Pennsylvania Department of Transportation PO Box 2926 Harrisburg, PA 17120	U.S. Department of Transportation Federal Hwy. Administration Washington, DC 20590	13. Type of Report and Period Covered Interim Report
		14. Sponsoring Agency Code

15. Supplementary Notes

Prepared in cooperation with the United States Department of Transportation, Federal Highway Administration. From the study "High Cycle Fatigue of Welded Bridge Details".

16. Abstract

Unexpected fatigue cracking often occurs in a steel bridge superstructure under relatively few live load cycles due to the interaction of primary and secondary bridge components. The forces in the lateral bracing system of the George Wade Bridge which spans the Susquehanna River on Interstate 81 near Harrisburg, Pennsylvania are studied to aid in the future investigation of the potential for fatigue crack growth due to displacement-induced stresses.

The study consists of the determination of the lateral bracing system forces both experimentally in the field and through finite element method modelling.

The forces in the lateral bracing system members are relatively small. The potential for fatigue cracking induced by out-of-plane displacement of the girders due to the lateral bracing system cannot be determined utilizing the available models since the magnitude of force is small. While the computed values of the force in the lateral bracing system varies between the field measurements and the theoretical values, both sets are of the same order of magnitude.

17. Key Words	18. Distribution Statement
Lateral Bracing Forces, Fatigue, out-of-plane Distortion, Field Study, Finite Element Analysis	

19. Security Classif. (of this report)	20. Security Classif. (of this page)	21. No. of Pages	22. Price
unclassified	unclassified	40	

Form DOT F 1700.7 (8-72) Reproduction of completed page authorized

COMMONWEALTH OF PENNSYLVANIA

Department of Transportation

Research Division

Wade L. Gramling, P.E. - Chief Research Engineer
Istvan Janauschek, P.E. - Research Coordinator

Project 72-3: High Cycle Fatigue of Welded Bridge Details

COMPARISON OF MEASURED AND THEORETICAL FORCES IN LATERAL BRACING MEMBERS

by

Dennis R. Mertz
J. Hartley Daniels

LEHIGH UNIVERSITY

Office of Research

Bethlehem, Pennsylvania

July 1981

Fritz Engineering Laboratory Report No. 386-6(81)

TABLE OF CONTENTS

1. INTRODUCTION

1.1 Background

Unexpected fatigue cracking often occurs in a steel bridge superstructure under relatively few live load cycles. Fatigue cracking commonly occurs in the vicinity of connections between primary and secondary components such as main girders and lateral bracing. It is also common in the vicinity of connections between primary bridge components such as main girders and floor beams.[1,2]

An example of the interaction of primary and secondary bridge components is shown in Fig. 1. Vehicular loads on the bridge deck can produce displacement of the lateral bracing member. If the transverse connection plate is not attached to the flange this displacement can produce an out-of-plane distortion of the girder web as shown in the figure. In the figure δ is the relative displacement of the girder flange with respect to the bottom of the transverse connection plate over the gap length. If the gap length is short, high web bending stresses may result, leading to reduced fatigue life of the girder.[2,3] A similar situation can also occur at the top flange and may even lead to higher web bending stresses if the flange is laterally supported by embedment in a concrete slab. Although this type of problem is more prevalent in welded members, it has also been observed in riveted structures.[1,4]

The occurrence of high secondary stresses near attachments such as shown in Fig. 1 normally go undetected during bridge design as a direct result of the simplified analyses normally used. In a steel girder-floorbeam-stringer superstructure, for example, each member is analyzed for flexure and shear stresses assuming planar behavior of the member.

The members are then connected together without a further analysis of the now three dimensional superstructure. This procedure is conservative with respect to static behavior but may be highly unconservative with respect to fatigue behavior. In addition to the stresses resulting from the three dimensional behavior of the superstructure, localized stresses occur in the vicinity of attachments and connections, such as shown in Fig. 1, which are highly sensitive to the type of connection used.

1.2 Objective and Purpose

The objective of this investigation is to study the forces in the lateral bracing system of the George Wade Bridge which spans the Susquehanna River on Interstate Route 81 near Harrisburg, PA. The bridge is one of a twin bridge structure consisting of a 34 span girder bridge, with the girders continuous over four or five spans, and ten approach spans.

The study was confined to the 136 foot second span of the continuous girder on the south end of the northbound bridge between piers 8 and 9 as shown in Fig. 2. This span was near a power source and was readily accessible. The span has two traffic lanes and an acceleration lane following an entrance ramp. The test lanes discussed in Chap. 3 are shown in the figure.

The purpose of the study of the lateral bracing forces is twofold:

(1) To ascertain the magnitude of the bracing forces to aid in the future determination of the potential for fatigue crack growth in such bridge details.

(2) To determine the magnitude of the forces in the lateral bracing system which indicates the degree to which the span under investigation functions as a three dimensional box section under truck loads.

1.3 Scope

The scope of this investigation is limited to the determination of the forces in the components of the lateral bracing system at one critical cross section. This cross section is at panel point 11 indicated in Figs. 2 and 3. The forces in the members are determined experimentally both in the field and through finite element method (F.E.M.) modeling. The significance of the effect of the resultant forces on the web gap stresses can then be assessed on the basis of the experimental and analytical studies in future investigations.

2. DESCRIPTION OF INSTRUMENTATION AND STRAIN RECORDING SYSTEM

2.1 Instrumentation of Bridge

Figure 3 shows the instrumentation used. A total of 6, 120 ohm, ¼-inch long electrical resistance, temperature compensating strain gages are located near panel point 11. One cross section of each of the two bracing members of the lateral system at this location is gaged a distance 12 in. from the edge of the bottom flange lateral connection plate. The gages are mounted in the longitudinal direction of the member. A quarter-bridge, three-wire hookup is used automatically providing lead-wire length compensation. Other gages were installed on the floorbeam tie plate connection to the longitudinal girders prior to placing the concrete deck. Unfortunately, these gages were destroyed during construction and no measurements were obtained.

2.2 Strain Recording System

The Federal Highway Administration's automatic data acquisition system shown schematically in Fig. 4 was used to record strains. This system, housed in a van, consists of an amplifer, an analog-to-digital signal converter, a computer and a teletype machine. As shown in the figure, ultraviolet analog trace recordings of live load variation of strain with time are made along with digitized strain signals recorded on magnetic tape. The strain signal is not continuously recorded due to limited traffic. Triggering of the recording system is done manually when truck traffic crosses the bridge.

3. FIELD INVESTIGATION

3.1 Loading Conditions

Strains were measured under two types of loading conditions: known loads and random loads. The known loads consist of the axle loads from the FHWA calibration truck shown in Fig. 5. Strains are recorded with the truck crossing the bridge in each of the three test lanes indicated in Fig. 2 at speeds of 10 and 20 mph. The prescribed use of the FHWA truck permitted magnitudes of live load strain to be related to a known loading condition. Measurements of live load strain under random loads in the form of normal traffic conditions proved inconsequential due to an extremely limited truck traffic volume during the field testing.

3.2 Strain Record

A portion of a typical analog trace of strain versus time generated on ultraviolet recording paper is shown in Fig. 6. Strain is recorded vertically and time horizontally to the scales shown. Traces marked Gage A and Gage B correspond to gages shown in Fig. 3. In Fig. 6, position 8 corresponds to the approximate location of the front wheels of the test truck (Fig. 5) passing over pier 8, where the truck is moving from left to right in the figure. Position 9 corresponds to the rear wheels leaving pier 9. The segment of interest therefore corresponds to the distance equal to the span length plus the truck length. Since the recording of strain is triggered manually, the exact location of the truck producing the maximum strain can only be approximated. The maximum strain is the product of the measured height from the trace times a conversion factor, which converts height to strain, times a calibration factor.

4. F.E.M. MODELLING OF THE BRIDGE

4.1 Assumptions

Other than the basic assumptions of structural analysis and the assumptions inherent to the finite element method (F.E.M.), further assumptions are made to simplify the finite element model. Exact modelling of the bridge requires many more computer resources in the stress analysis than are available or cost effective at the Lehigh University Computing Center. To reduce the required computer resources, the following additional assumptions are made.

1) As shown in Fig. 7, only four spans of the entire bridge are actually discretized. This model corresponds to the section of the bridge between piers 7 and 11 where hinges occur and in which strain measurements are made. Only the span between piers 8 and 9 containing panel point 11 is discretized in detail. A much coarser discretization is used in the other spans. Simple girders and a limited number of floorbeams are used to model these spans, so that the actual flexural and torsional continuity to the finely discretized span is simulated.

2) A typical cross section of the finely discretized span is shown in Fig. 8. It is assumed that this span, containing the panel point under investigation, can be realistically modelled using only three horizontal layers of nodal points. The top layer of nodal points corresponds to the mid-depth of the concrete deck. The bottom flange of the floorbeams is represented by a middle layer of nodal points, 79.5 in. below the top layer. The bottom layer of nodal points is 33.5 in. lower, corresponding to the bottom

flange of the main girders. Utilizing these three layers of nodal points to provide connectivity, structural components of the span are modelled. Since these layers do not correspond to all of the axes of all of the structural components, various transformations are performed on the components' actual section properties yielding fictitious, yet realistic, properties for the finite elements.

3) As discussed previously, the outside main girder of the finely discretized span is skewed approximately one degree in order to accommodate an entrance ramp. The local longitudinal axis of the skewed girder does not correspond to one of the chosen global axis, therefore the most convenient method of specifying boundary conditions about the global axis is not completely realistic. Since this girder is on the opposite side of the bridge from the point under investigation and this point is at mid-span, far from the boundary conditions, the assumption is made that boundary conditions about the global axes are satisfactory. The added complexity of skewing the boundary conditions is then eliminated.

4.2 Modelling Techniques

4.2.1 Girders and Floorbeams

Since out-of-plane movement of the girders and floorbeams is possible, the usual method of modelling flanges as simple truss elements and webs as plane stress elements is not realistic. In order to model the degrees of freedom associated with out-of-plane displacement, the flanges are represented by three-dimensional beam elements, combining axial stress with flexural stresses. The webs are modelled as plate bending elements, superimposing bending capabilities upon membrane stresses.

4.2.2 Lateral Bracing System and Description of Variations

The lateral bracing system connected to the main girders near the bottom flange acts as a horizontal truss. Therefore, the diagonal and transverse cross bracing members are modelled as simple truss elements. These are the members in which actual live load strains are measured and for which the model is designed to accurately predict.

A catwalk connecting the bracing system to the bottom flange of the floor beams, influences the behavior of the bracing members.

Four variations of the discretization of the catwalk in the overall structure are included. Variation 1 is the basic discretization as previously described, with no catwalk members present. For variations 2 and 3, vertical and then longitudinal catwalk members are added respectively. Variation 4 consists of the basic discretization with all catwalk members in place but with the strength of the concrete deck reduced to a negligible magnitude.

4.2.3 Boundary Continuity

Continuity of boundary conditions at piers 8 and 9 is maintained between the finely discretized span and the outer spans by the connection shown in Fig. 9. The three levels of nodal points in the inner span are connected together by a rigid link over the piers. This rigid link is in turn rigidly connected to the girders of the outer spans. As such, deformations and rotations are transferred from one type discretized span to the other.

4.3 Description of F.E.M. Model

4.3.1 Connectivity of Nodal Points

Detailed plan views of the finely discretized span consisting of three horizontal layers of nodal points are shown in Figs. 10, 11, and 12. Figure 10 shows the top layer of nodal points. Finite elements in the plane described by this layer represent the concrete deck, and the top flanges of the girders and floorbeams. The node lines labelled as piers 8 and 9 are where this span is rigidly connected to the coarsely discretized outer spans. Changes in main girder cross sections are shown as node lines marked with the symbol, Δ.

A plan view of the middle layer of nodal points is given in Fig. 11. Elements in this plane are beam elements along the center line of the floorbeams representing their flanges. Plate bending elements along the centerlines of the main girders and floorbeams represent the webs connecting this layer to the layer above.

Figure 12 shows the bottom layer of nodal points. Beam elements representing the main girder flanges, truss elements representing the lateral bracing members, and beam elements with transformed section properties calculated to simulate the catwalk are in this plane. The lower portion of the main girder webs are modelled as plate bending elements connecting this layer to the layer immediately above. Additional beam elements representing the catwalk system connect the lateral bracing system to the floorbeam flanges above along the catwalk centerline.

4.3.2 Loading Conditions

Figure 13 shows a schematic diagram of the 15 positions of the FHWA calibration truck statically analyzed using the SAP IV. The 15 loading conditions comprise a matrix of 3 transverse locations by 5 longitudinal locations across the span.

Since concentrated loads are most easily modelled as nodal point loads, the six tire patch loads were reduced to the three axle loads shown in Fig. 5. The longitudinal node lines nearest the center of each test lane (see Fig. 2) are assumed to be the test lane centerlines. The longitudinal line of axle loads was then placed along the assumed lane centerlines with the drive axle at the five arbitrarily chosen transverse node lines shown in Fig. 13. The truck axles loads were placed to simulate the test configuration of the truck moving from pier 7 toward pier 11. Using a simple lever rule, the axle loads are proportioned to nodes along the assumed lane centerlines. From the resultant output, bracing member force vs. longitudinal truck location can be plotted and maximum force determined.

5. RESULTS OF INVESTIGATION

5.1 Calculated Lateral Bracing Member Forces

Sample calculations of the axial force in the lateral bracing members made from recorded strains are shown in Appendix A. Maximum strain recorded under the specified loading conditions is converted to stress by multiplying by Young's modulus of elasticity. Inherent with this procedure is the assumption that the members are under pure axial load. The resulting stresses are averaged over the web and flange. Through integration of these average stresses over the cross sectional area, maximum load is determined.

Utilizing the technique described above, maximum forces for the lateral bracing members at panel point 11 are calculated. The maximum forces with the calibration truck in each of the three lanes are shown in Table 1. The maximum force in the cross bracing member varies from -1.5 kips to 7.0 kips producing a force range of 8.5 kips. For the diagonal bracing member, the force varies from -1.5 kips to 1.0 kip, for a force range of 2.5 kips.

5.2 Results of the Finite Element Analysis

The axial forces in the lateral system as calculated using SAP IV[5] for variations 1 through 4 (Art. 4.2.2) are shown in Tables 2, 3, 4, and 5. From the force versus longitudinal location of the truck in the lane shown in the tables, maximum forces can be extrapolated. The approximate maximum forces obtained from the F.E.M. results are shown in Table 6.

5.3 Comparison of F.E.M. and Field Investigation Results

The results from the F.E.M. analyses and the field investigations are in agreement in that all the calculated forces are extremely low in magnitude. However, large differences in these small magnitude values are seen between the F.E.M. and field results. While the cross bracing compression forces are basically comparable in both the F.E.M. and field results, the cross bracing tension forces in the F.E.M. analyses fall far below the 7.0 kips observed in the field. The compression and tension forces in the diagonal bracing members from the F.E.M. analyses are two- or threefold greater than those observed in the field.

6. CONCLUSIONS

The results of the F.E.M. analyses and the field investigations are not as close to each other in magnitude as had been anticipated. Originally, it was anticipated that the F.E.M. analyses would simulate the actual bridge behavior such that only small differences in the calculated and measured values would be observed. Then, the various parameters, such as the stiffnesses of the bridge components, could be varied in the model to study the effects. In actuality, while both phases of the investigation yield small forces in the lateral system members, significant differences between the values of both phases are evident.

The differences between the calculated and measured values indicates that the model is not sensitive enough to yield more equal results. It is, however, accurate enough to produce forces of the same order of magnitude as those measured.

Under vehicular loads, the bridge's lateral system is loaded through lateral displacement of the main girder bottom flanges. It has been shown through both phases of this investigation that relatively small forces exist in the lateral system members.

The conclusions drawn from the study of the lateral bracing forces can be summarized as follows:

(1) The magnitude of the axial forces in the lateral bracing system is relatively small. The effect of these small forces on the potential for fatigue cracking must still be evaluated.

(2) The degree to which the span investigated functions as a three dimensional box section under truck loads appears to be relatively small.

7. ACKNOWLEDGMENTS

This study is part of PennDOT Research Project No. 72-3, a study of high cycle fatigue of welded details, sponsored by the Pennsylvania Department of Transportation and the U.S. Department of Transportation - Federal Highway Administration.

The authors wish to gratefully acknowledge the assistance of the staff at Fritz Engineering Laboratory in the preparation of this report. Thanks are due Mr. Hugh T. Sutherland for his assistance in the acquisition of test data. A number of Fritz Engineering Laboratory staff under the supervision of Mr. K. R. Harpel assisted with the field work. The manuscript was prepared by Miss Shirley Matlock. The figures were drafted by Mr. John Gera and Mrs. Sharon Balogh. Special thanks are also due Mr. Hans Out for his help in field data reduction. Finally the guidance and helpful suggestions of Dr. John W. Fisher are gratefully appreciated.

8. TABLES

TABLE 1

Measured Bracing Member Forces

Lane Occupied	Cross Bracing Force (kips)	Diagonal Bracing Force (kips)
1	1.50 compression	1.50 compression
2	5.50 tension	1.00 tension
3	7.00 tension	0.50 tension

TABLE 2

Axial Forces from Variation No. 1
(kips)

Lane Loaded	Position in Lane	Cross Bracing @ Panel Point 11					Diagonal Bracing @ Panel Point 11				
		1	2	3	4	5	1	2	3	4	5
1		-0.044	-0.676	-1.416	-1.593	-0.957	-1.419	-2.230	-1.878	-0.269	0.439
2		0.039	0.571	1.631	1.097	-0.084	0.448	0.814	1.004	1.106	2.250
3		0.052	0.834	2.040	1.892	0.678	-0.039	-0.072	0.156	0.027	0.024

TABLE 3

Axial Forces from Variation No. 2
(kips)

Lane Loaded	Position in Lane	Cross Bracing @ Panel Point 11: 1	2	3	4	5	Diagonal Bracing @ Panel Point 11: 1	2	3	4	5
1		0.123	-0.102	-0.470	-0.750	-0.535	-1.518	-2.238	-1.491	0.775	1.356
2		0.106	0.747	1.866	1.322	0.074	-0.585	-0.819	-0.541	0.100	0.311
3		0.017	0.633	1.655	1.602	0.599	0.194	0.295	0.055	-0.544	-0.477

TABLE 4

Axial Forces from Variation No. 3
(kips)

Lane Loaded	Position in Lane	Cross Bracing @ Panel Point 11					Diagonal Bracing @ Panel Point 11				
		1	2	3	4	5	1	2	3	4	5
1		0.356	0.281	-0.172	-0.745	-0.616	-2.203	-3.384	-2.373	0.801	1.615
2		0.398	1.127	2.002	1.171	-0.003	-1.424	-0.912	-0.786	0.753	0.606
3		0.264	0.961	1.781	1.454	0.510	-0.494	-0.600	-0.112	0.145	-0.098

TABLE 5

Axial Forces from Variation No. 4
(kips)

Lane Loaded	Position in Lane	Cross Bracing @ Panel Point 11					Diagonal Bracing @ Panel Point 11				
		1	2	3	4	5	1	2	3	4	5
1		-0.321	-0.782	-1.146	-1.362	-1.039	-0.893	-1.080	0.220	2.939	3.033
2		-0.104	0.315	1.193	0.704	-0.119	-0.483	-0.521	0.513	1.704	1.084
3		0.054	0.604	1.413	1.332	0.639	-0.200	-0.246	0.107	0.169	-0.274

TABLE 6

Variation No.	Cross Bracing Force (kips) Minimum	Cross Bracing Force (kips) Maximum	Diagonal Bracing Force (kips) Minimum	Diagonal Bracing Force (kips) Maximum
1	1.6 compression	2.1 tension	2.3 compression	2.3 tension
2	0.8 compression	2.0 tension	2.3 compression	0.4 tension
3	0.8 compression	2.1 tension	3.4 compression	0.8 tension
4	1.5 compression	1.4 tension	1.1 compression	3.1 tension

(Refer to Art. 4.2.2 for description of the four variations)

9. FIGURES

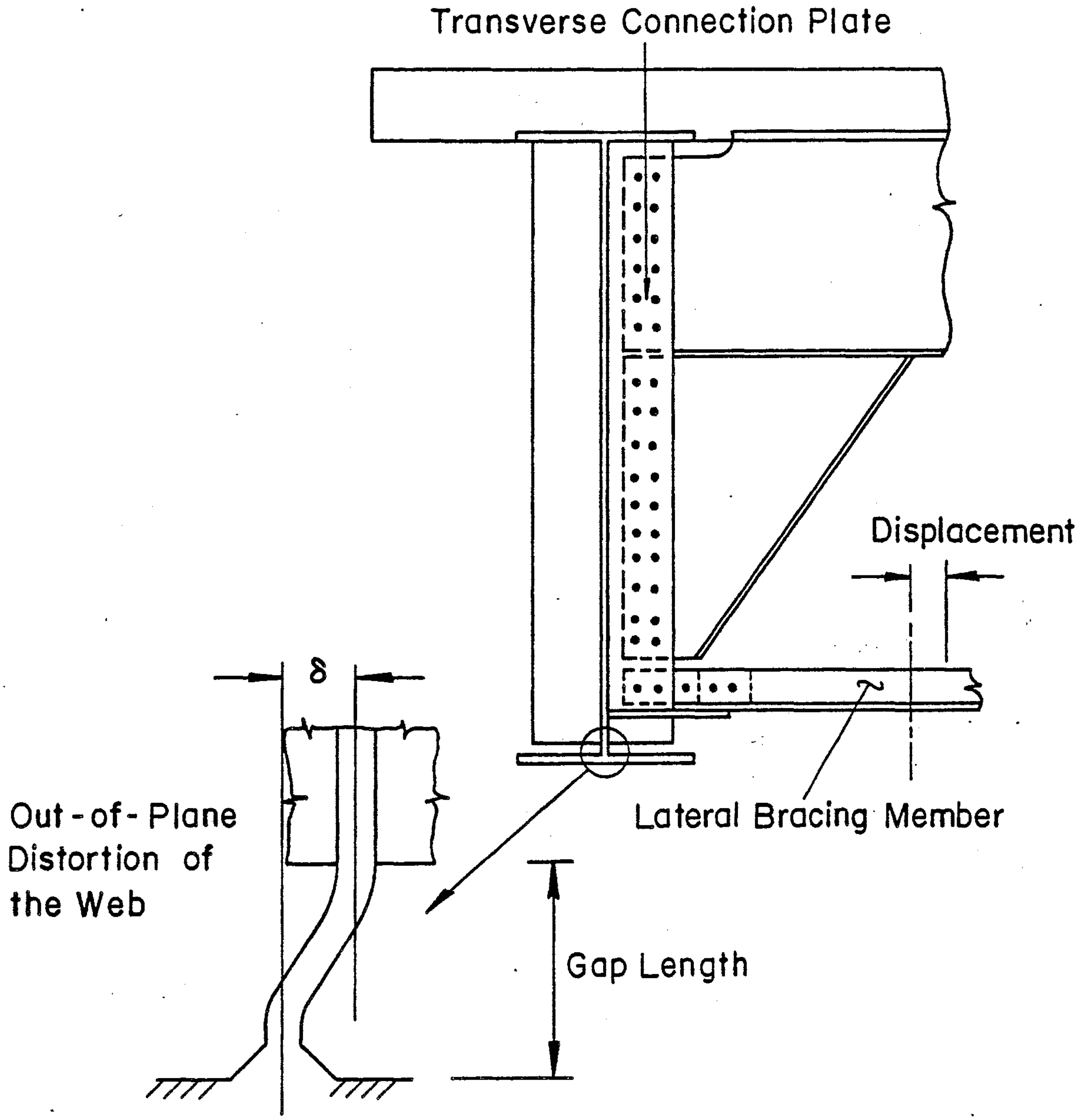

Fig. 1 Schematic of Transverse Connection Plate Showing Possible Distortion of the Web in Positive Moment Region due to Lateral Bracing Member Displacement, δ

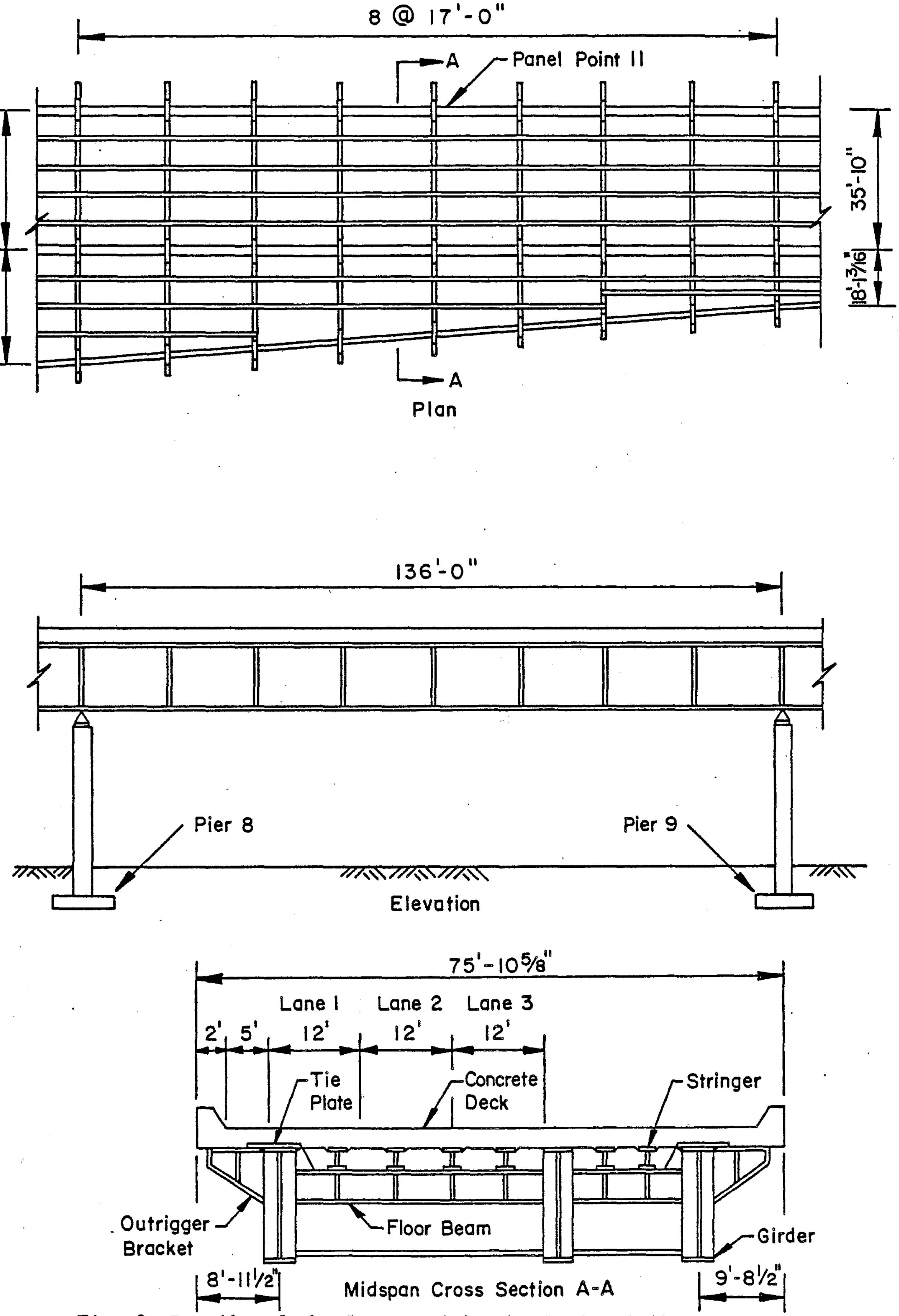

Fig. 2 Details of the Span used in the Study, Indicating the Location of Panel Point 11 (see Fig. 3)

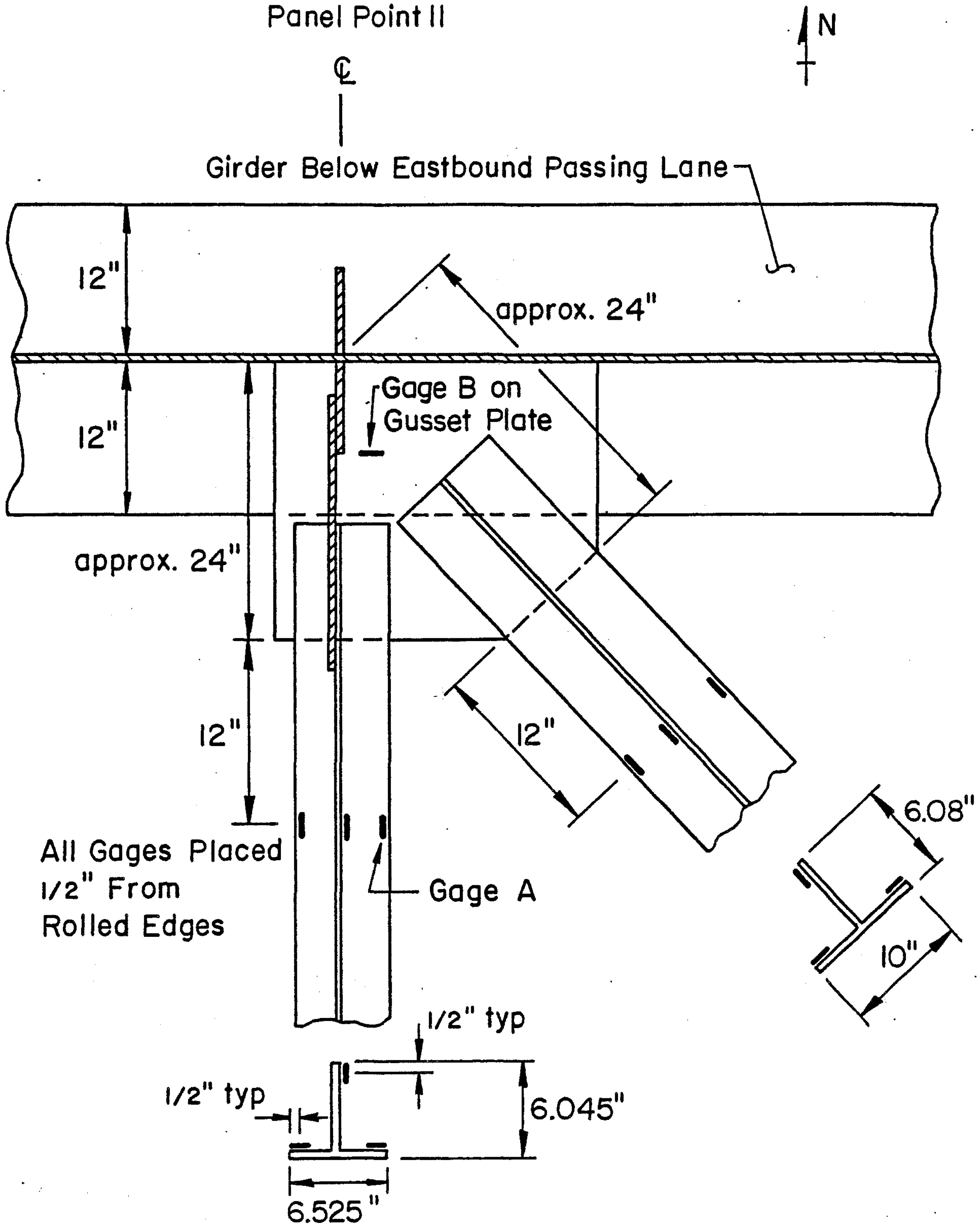

Fig. 3 Details of Panel Point 11 (see Fig. 2) and Instrumentation Used

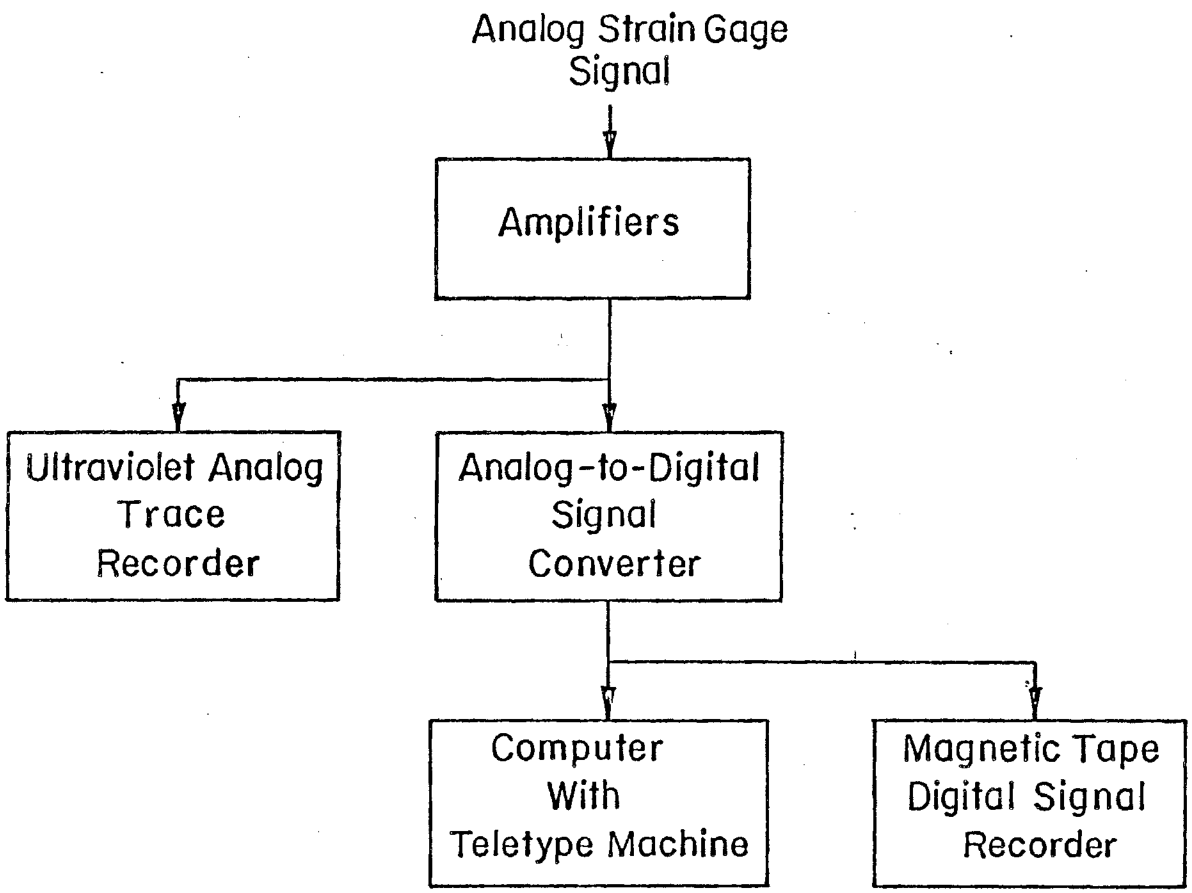

Fig. 4 Automatic Data Acquisition System

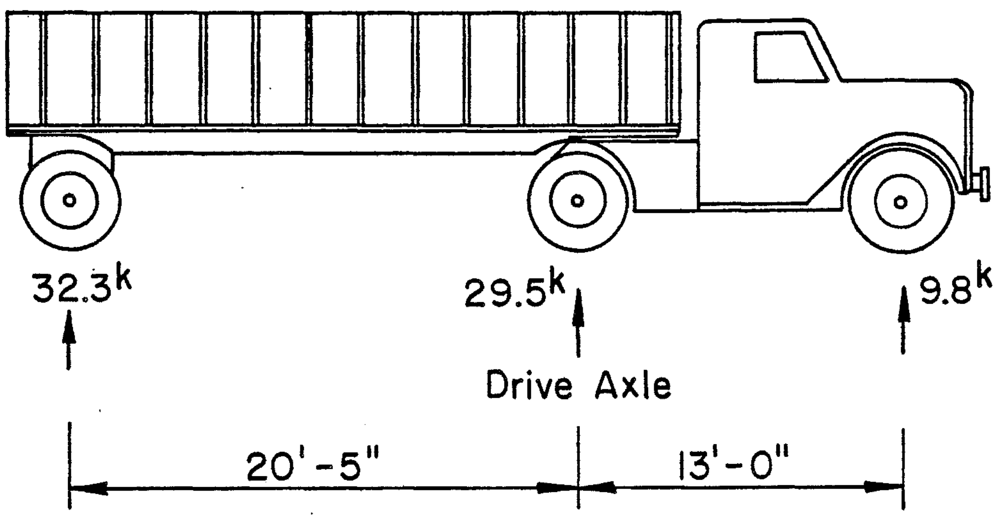

Fig. 5 Federal Highway Administration Calibration Truck

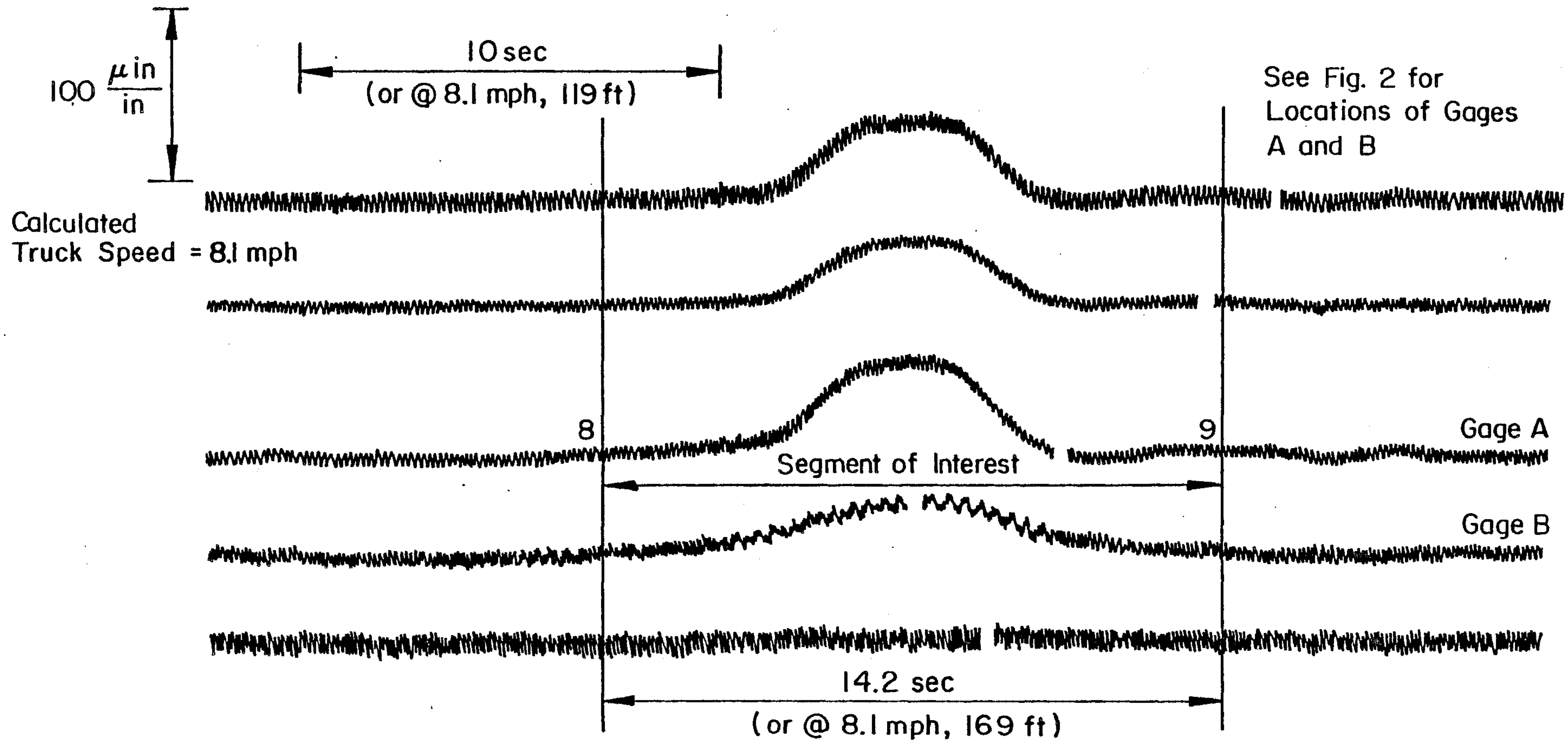

Fig. 6 Typical Analog Trace of Strain versus Time

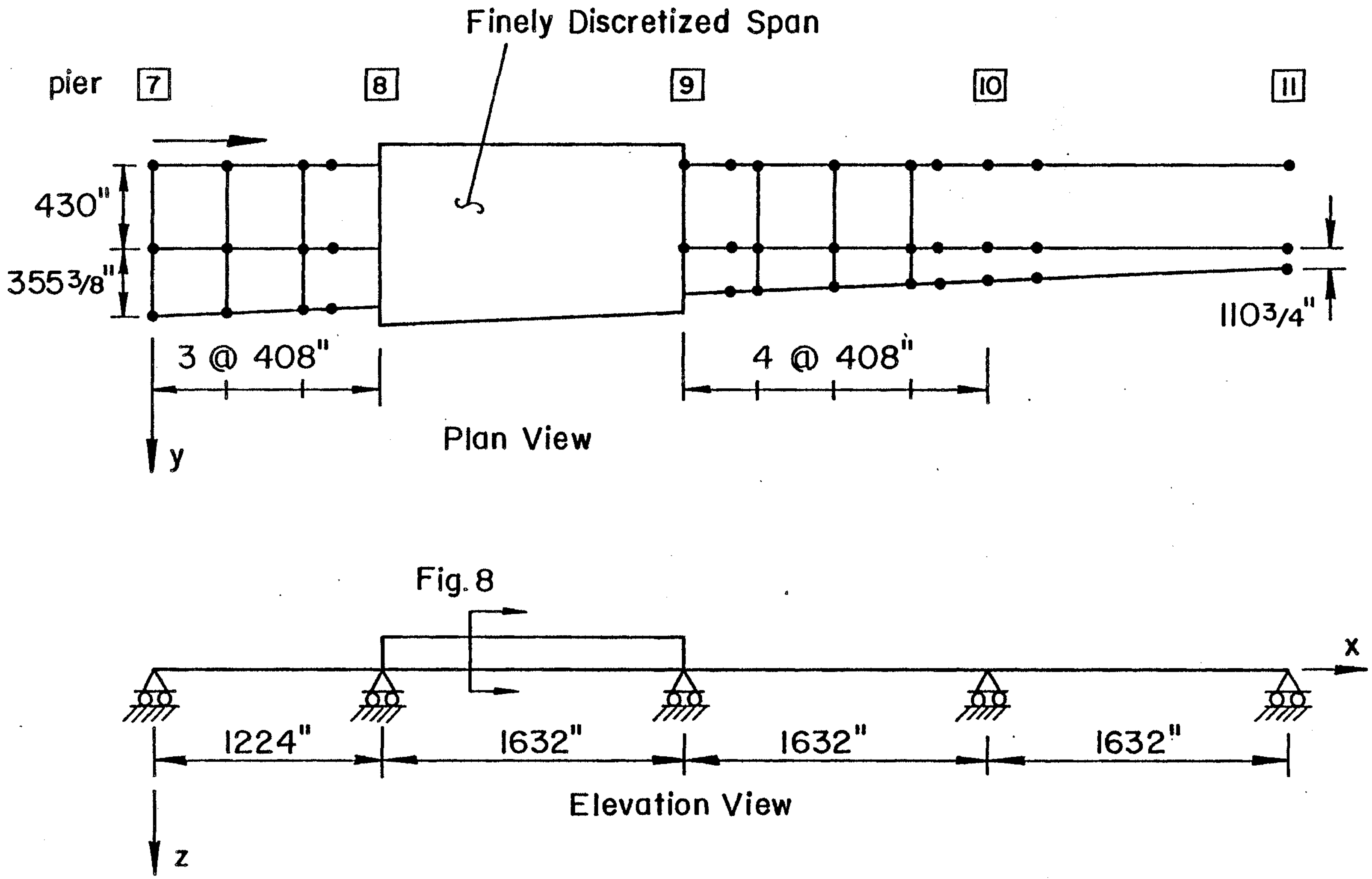

Fig. 7 Overall Bridge Discretization

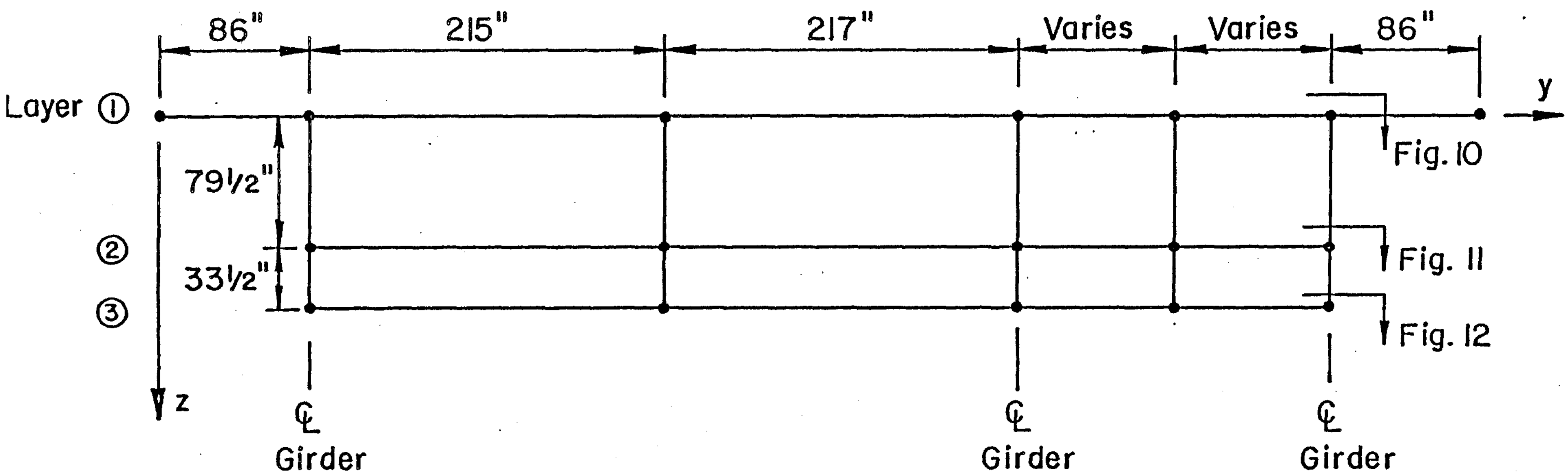

Fig. 8 Typical Cross Section of Finely Discretized Span

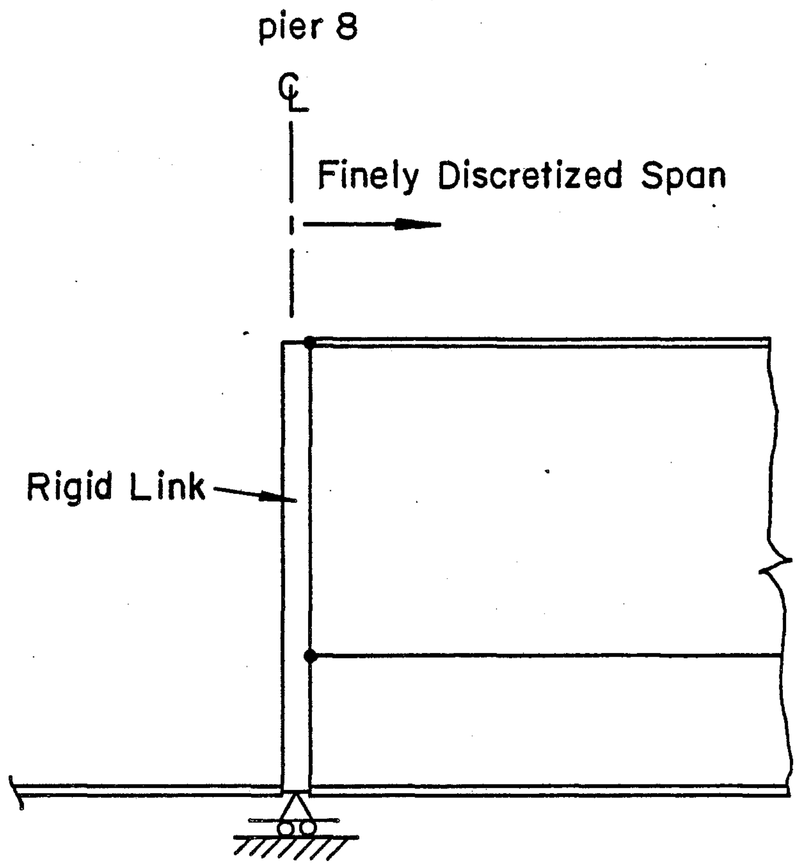

Fig. 9 Discretized Connection between Finely Discretized Span and Outer Spans

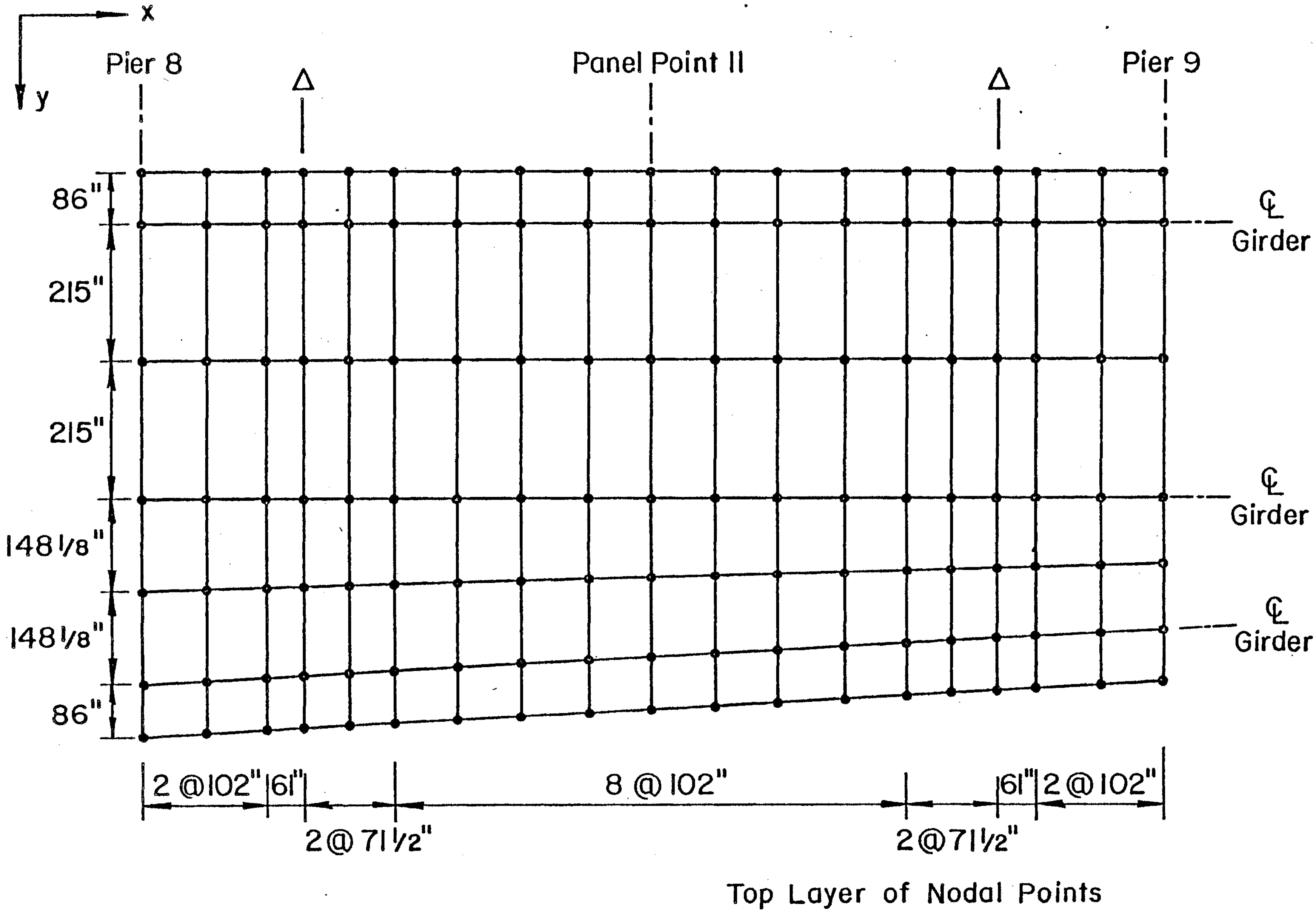

Fig. 10 Plan View of Top Layer of Nodal Points in Finely Discretized Span

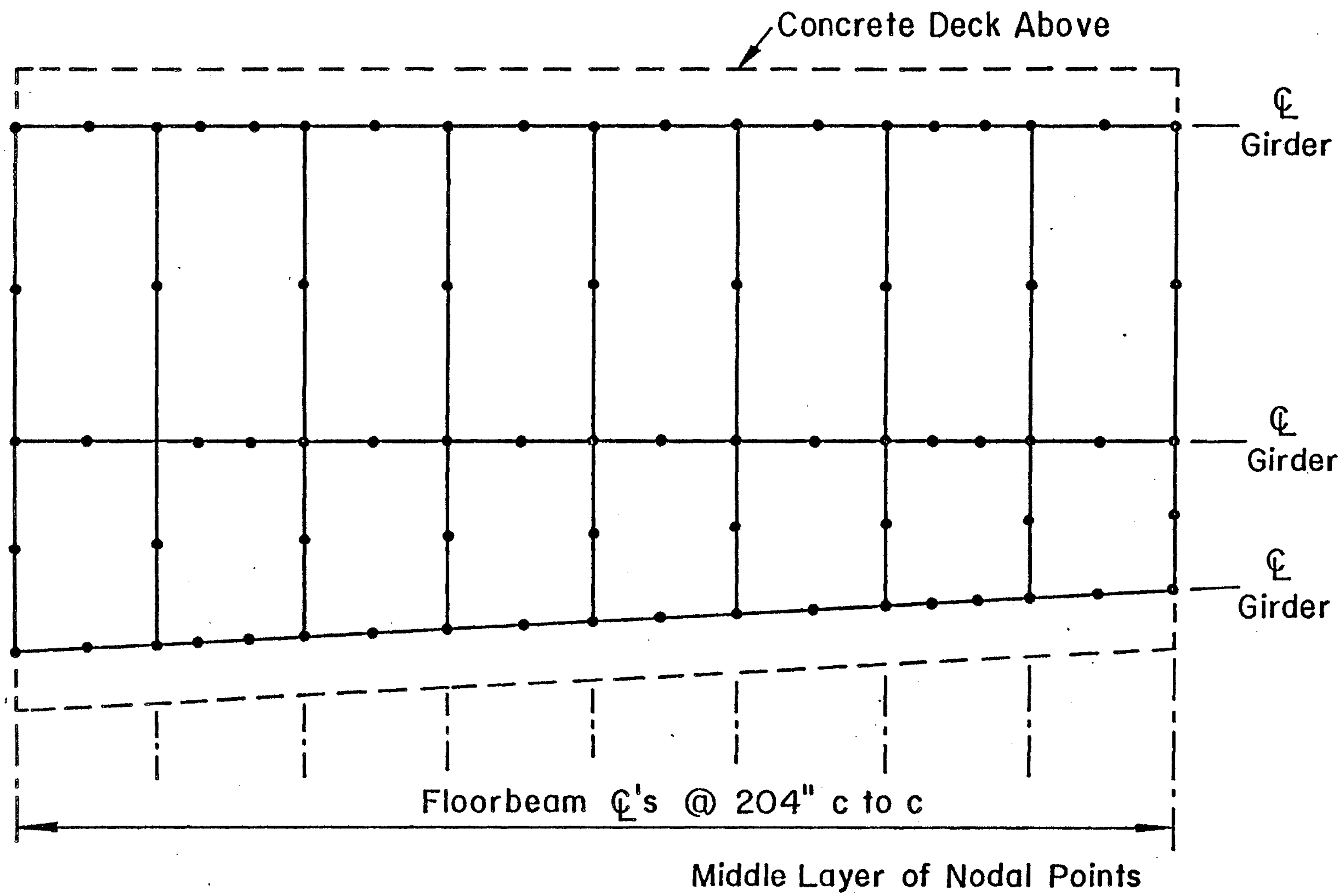

Fig. 11 Plan View of Middle Layer of Nodal Points in Finely Discretized Span

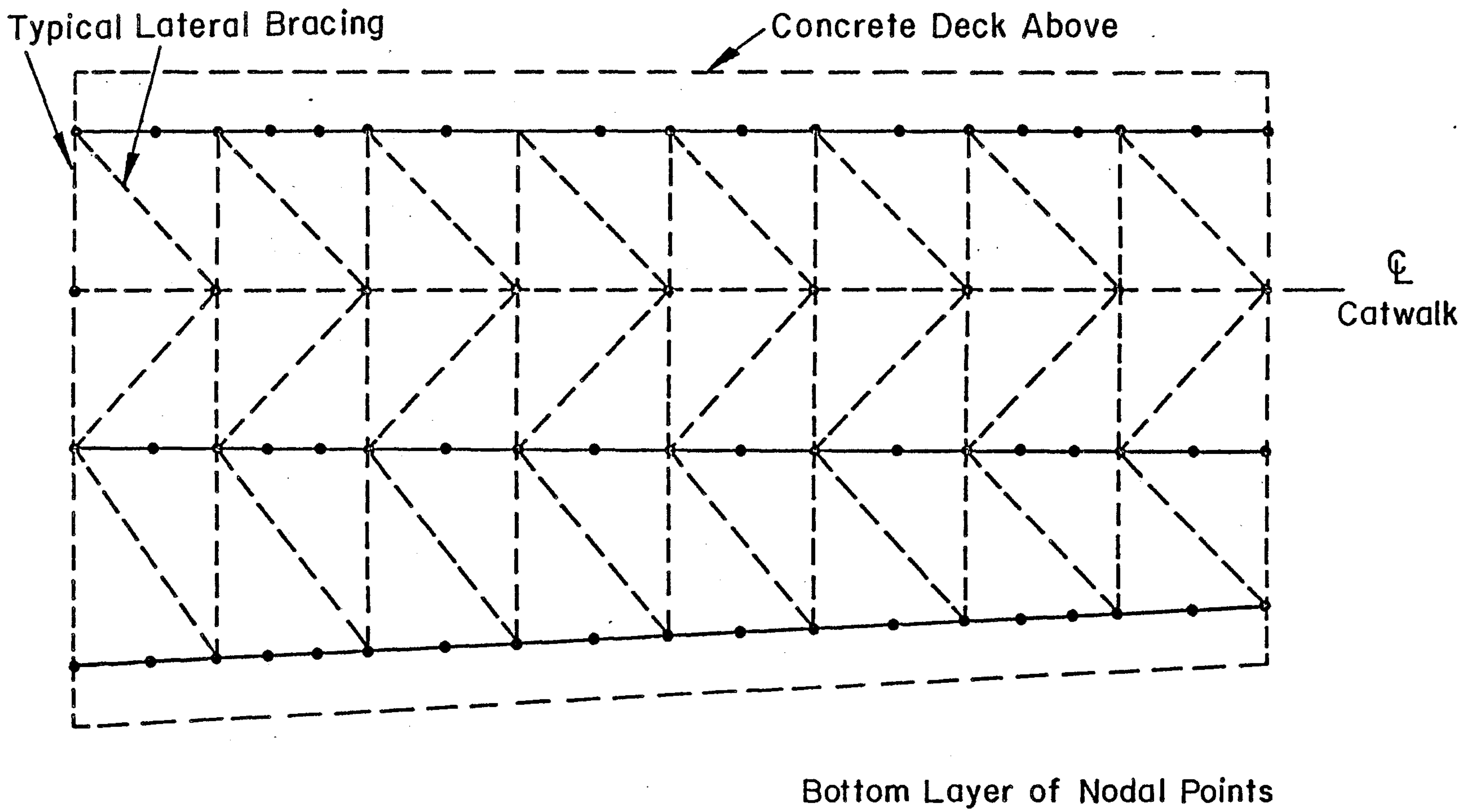

Fig. 12 Plan View of Bottom Layer of Nodal Points in Finely Discretized Span

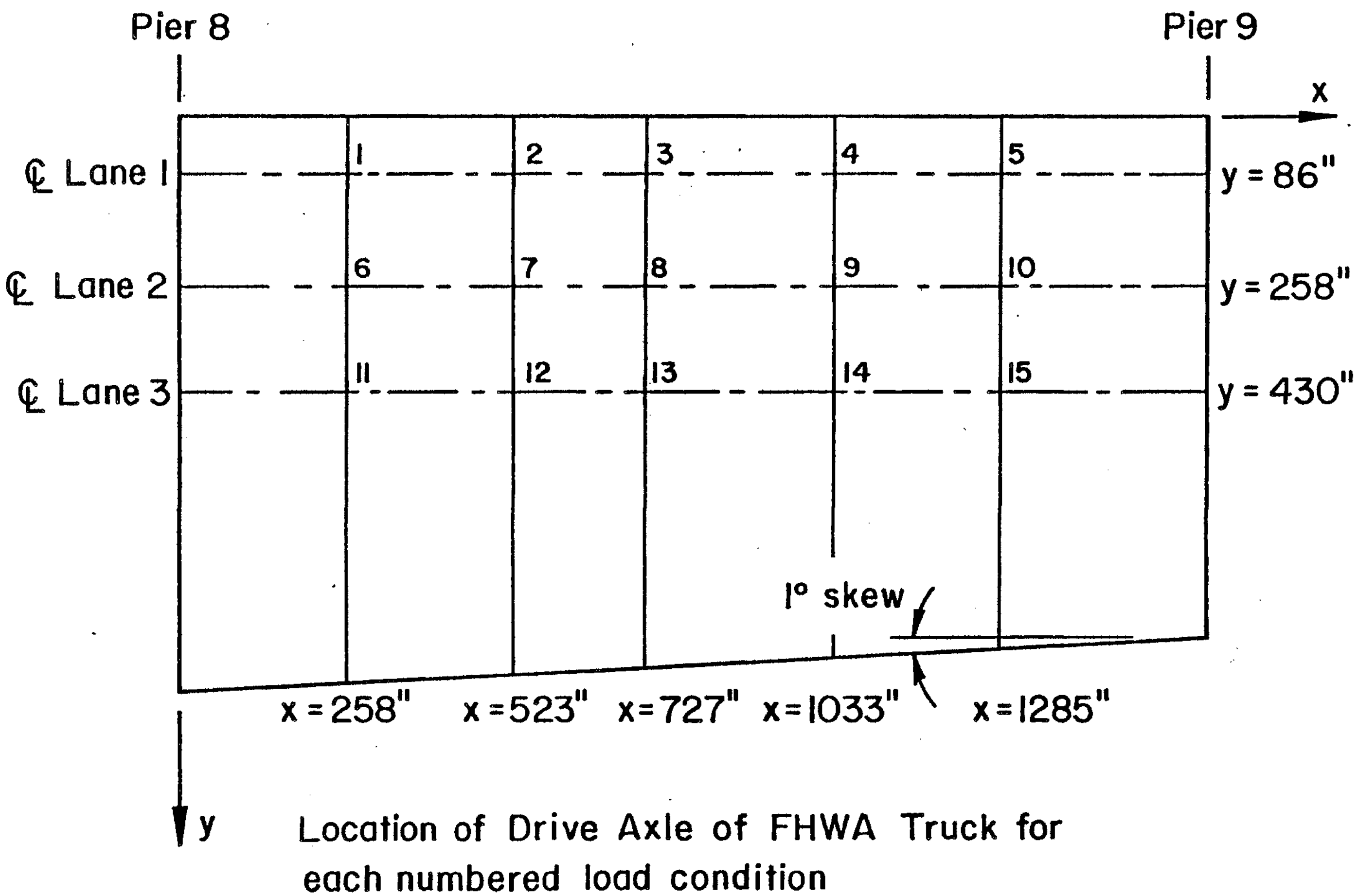

Fig. 13 Matrix of FHWA Truck Locations for the Static Load Conditions

10. REFERENCES

1. Fisher, J. W.
BRIDGE FATIGUE GUIDE - DESIGN AND DETAILS, American Institute of Steel Construction, Booklet T112-11/77, New York, 1977.

2. Fisher, J. W.
FATIGUE CRACKING IN BRIDGES FROM OUT-OF-PLANE DISPLACEMENTS, The Canadian Journal of Civil Engineering, Vol. 5, No. 4, 1978.

3. Fisher, J. W., Hausammann, H., Sullivan, M. D. and Pense, A. W.
DETECTION AND REPAIR OF FATIGUE DAMAGE IN WELDED HIGHWAY BRIDGES, NCHRP 206, Transportation Research Board, Washington, D.C., June 1979.

4. Fisher, J. W.
INSPECTING STEEL BRIDGES FOR FATIGUE DAMAGE, Fritz Engineering Laboratory Report No. 386-15(81), Lehigh University, March 1981.

5. Bathe, K-J., Wilson, E. L. and Peterson, F. E.
SAP IV, A STRUCTURAL ANALYSIS PROGRAM FOR STATIC AND DYNAMIC RESPONSE OF LINEAR SYSTEMS, EERC 73-11, Earthquake Engineering Research Center, University of California, Berkeley, California, June 1973.

11. APPENDIX

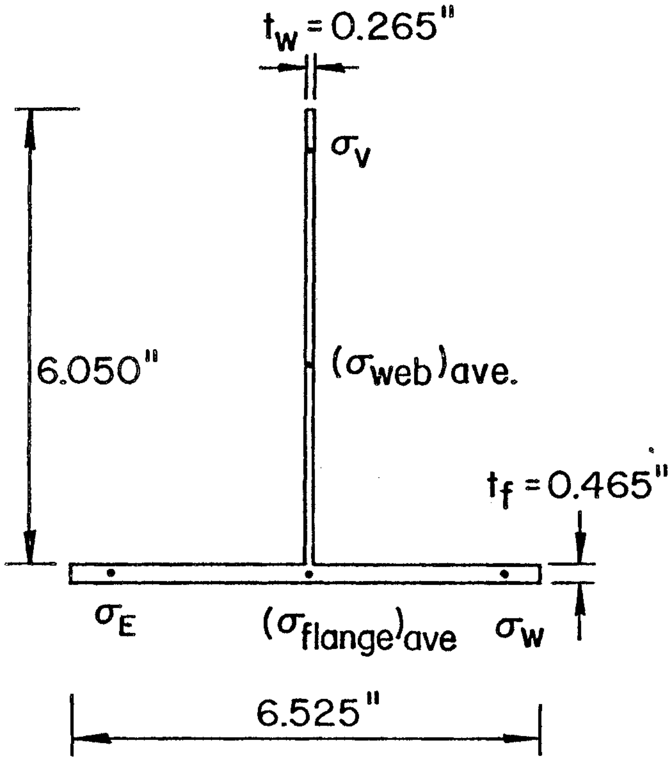

Calculation of Lateral Bracing Force

σ_E = 1.38 ksi

σ_W = 1.91 ksi   calculated from recorded maximum strains

σ_V = 2.40 ksi

$$(\sigma_{flange})_{ave} = \frac{1}{2}(\sigma_E + \sigma_W) = 1.65 \text{ ksi}$$

$$(\sigma_{web})_{ave} = \frac{1}{2}[\sigma_V + (\sigma_{flange})_{ave}] = 2.03 \text{ ksi}$$

P = (1.65 ksi)(6.525")(0.465")

+ (2.03 ksi)(6.050")(0.265")

P = 8.25 kips

DISCLAIMER

Prepared in cooperation with the Pennsylvania Department of Transportation and the U. S. Department of Transportation, Federal Highway Administration. The contents of this report reflect the views of the authors who are responsible for the facts and the accuracy of the data presented herein. The contents do not necessarily reflect the official views or policies of the Pennsylvania Department of Transportation or the U. S. Department of Transportation, Federal Highway Administration. This report does not constitute a standard, specification or regulation.